Available online at www.sciencedirect.com

ScienceDirect

Proceedings of the Combustion Institute 000 (2022) 1–8

Proceedings of the Combustion Institute

www.elsevier.com/locate/proci

Experimental investigation of non-equilibrium plasma-assisted ammonia flames using NH_2* chemiluminescence and OH planar laser-induced fluorescence

Jinhoon Choe [a], Wenting Sun [a,b,*]

[a] School of Mechanical Engineering, Georgia Institute of Technology, Atlanta, GA 30332, United States
[b] School of Aerospace Engineering, Georgia Institute of Technology, Atlanta, GA 30332, United States

Received 4 January 2022; accepted 1 July 2022
Available online xxx

Abstract

This study investigates the effect of nano-second pulsed non-equilibrium plasma on ammonia combustion in a model gas turbine combustor using NH_2* chemiluminescence and OH planar laser-induced fluorescence (PLIF). Nano-second pulsed plasma discharge is generated at the exit of the premixed ammonia/air mixture injection tube. Broadband chemiluminescence observation shows that plasma can improve the stabilization of ammonia/air flame and extend the attached flame regime to a lower equivalence ratio. To understand the coupling effect between plasma kinetics and flame dynamics, NH_2* chemiluminescence and OH PLIF of ammonia/air flames are measured at different conditions. With the increase of discharge voltage or discharge power, both NH_2* chemiluminescence intensity and OH PLIF signal intensity increase, and this observation may explain the improved stabilization of ammonia flames. At very lean condition (equivalence ratio between 0.48 and 0.57, no visible flame existed), both NH_2* chemiluminescence and OH PLIF signal are observed in the proximity of electrode region with plasma activation. If air is replaced by pure nitrogen (N_2), NH_2* chemiluminescence is measurable but extremely weak. As the oxygen (O_2) concentration in the oxidizer stream gradually increases, NH_2* chemiluminescence intensity increases linearly with O_2 concentration under plasma activation. This finding indicates that the NH_2* production in plasma-assisted ammonia oxidation process is possibly related to the production of OH or oxygen-related species. The direct electron impact on NH_2* production might be secondary.

Keywords: Plasma-assisted combustion; Ammonia combustion; NH_2* chemiluminescence, OH planar laser-induced fluorescence

* Corresponding author at: School of Aerospace Engineering, Georgia Institute of Technology, Atlanta, GA 30332, United States.
E-mail address: wenting.sun@aerospace.gatech.edu (W. Sun).

https://doi.org/10.1016/j.proci.2022.07.001
1540-7489 © 2022 Published by Elsevier Inc. on behalf of The Combustion Institute.

1. Introduction

The idea of using ammonia (NH_3) as a fuel started in the 1960s [1,2]. Verkamp et al. [3] studied minimum ignition energies and quenching distances for ammonia/air mixtures. They concluded that pure ammonia could not be used as fuel for gas turbines due to its poor flame stability. Because of the narrow flammability range and high NO_x emission [4], ammonia combustion was then forgotten for several decades. As the problem of global warming becomes more intense and alternative zero-carbon fuel is urgently needed, ammonia has drawn attention again to be an alternative fuel.

Recently, Kurata et al. [5] demonstrated an ammonia-fueled micro gas turbine using non-premixed combustor to improve ammonia flame stability. Since the ignition of pure ammonia flame was challenging, the initial start-up of the combustor was conducted by using kerosene, and the kerosene was then gradually replaced by ammonia. A selective catalytic reduction (SCR) system was installed at the turbine outlet to remove NO_x in the exhaust because NO emission was high (over 1100 ppm at 16% O_2) compared to a typical dry low NO_x combustor using carbon-based fuels. Valera-Medina et al. [6] investigated ammonia/methane/air flames in a premixed swirl burner. They reported that a high swirl number is inappropriate for premixed ammonia/methane flames owing to the unsteadiness of flame and suggested using a swirler with a lower swirl number. Pugh et al. [7] studied premixed ammonia/hydrogen/air flames in a turbulent swirl burner. The fuel consisted of 70% ammonia and 30% hydrogen by mole fraction. From emissions measurement, they found that NO_x emissions were sensitive to the equivalence ratio (ϕ) and reactant humidification could reduce NO_x emission. Pugh et al. [8] investigated NO emission and OH^*, NH_2^* chemiluminescence of premixed and non-premixed ammonia/air flames. They reported a complementary relationship between a decrease in OH^*, an increase in NH_2^*, and the reduction of measured NO as the equivalence ratio increased. Later, Pugh et al. [9] further investigated OH^*, NH_2^*, and NH^* chemiluminescence of the premixed and non-premixed ammonia/air flames at elevated pressures and temperature conditions. They found that higher NH_2^* chemiluminescence intensity is a good marker of NO reduction. In summary, two outstanding challenges of ammonia combustion are difficulty in flame stabilization and high NO_x emission.

From another perspective, non-equilibrium plasma has been widely used to enhance flame stabilization for a variety of hydrocarbon fuels [10–13]. To understand the mechanism of plasma-assisted flame stabilization, OH planar laser-induced fluorescence (PLIF) was typically employed as OH radical could enhance flames. For example, in a bluff-body stabilized propane/air flame, Lacoste et al. [14] measured OH PLIF with nano-second pulsed plasma. They found that plasma increased the OH fluorescence signal in the discharge area and caused a significant reduction in the liftoff height. In the presence of microwave plasma, Rajasegar et al. [15] studied premixed methane/air flames in a swirl-stabilized dump combustor. They observed a significant extension on the lean blowoff limit and enhanced flame stabilization. The OH PLIF study showed that OH number density increased up to 150% with plasma. Similar observation on flame enhancement was reported by Choe and Sun [10] and they also found that plasma could increase NO_x emission.

In the past, almost all plasma-assisted combustion studies focused on carbon-based fuels or hydrogen. Recently, researchers have started to consider the potential effect of plasma on ammonia combustion. Shioyoke et al. [16] conducted numerical simulation and reported the increase in laminar burning velocity of ammonia flames with addition of plasma generated species (H, O and OH). They concluded that the increase in OH produced by plasma accelerated flame propagation. Faingold and Lefkowitz [17] numerically studied ignition delays of ammonia/oxygen/helium mixtures and reported reduced ignition delays under plasma activation owing to plasma created species (H, O and OH).

In a very recent work by Choe et al. [18], plasma-assisted ammonia flame was first experimentally investigated. Simultaneous reduction of NO_x emission and extension of lean blowoff limits of ammonia/air flames with the activation of nano-second pulsed plasma were reported. This observation makes the application of plasma in ammonia combustion become very promising. Since this topic is still in its infancy and only a handful relevant work exists, the mechanism of NO_x reduction and flame enhancements in ammonia combustion with plasma activation is largely unknown. In this work, we will investigate the underlying mechanism of ammonia flame enhancement by nano-second pulsed plasma using NH_2^* chemiluminescence and OH PLIF.

2. Experimental setup

Fig. 1 depicts the swirl stabilized dump combustor integrated with nano-second pulsed plasma discharges. The discharge is generated between a center rod electrode and an outer ring electrode. Oxidizer and ammonia are premixed in the bottom of the combustor. As for oxidizer, air is primarily used to generate ammonia flames, and synthetic mixture of nitrogen (N_2) and oxygen (O_2) with different ratios is also employed to investigate the effect of oxygen concentration. Air, oxygen, nitrogen and ammonia are all research grade pure (from Airgas) and their flow rates are controlled using choked orifices.

Please cite this article as: J. Choe and W. Sun, Experimental investigation of non-equilibrium plasma-assisted ammonia flames using NH2* chemiluminescence and OH planar laser-induced fluorescence, Proceedings of the Combustion Institute, https://doi.org/10.1016/j.proci.2022.07.001

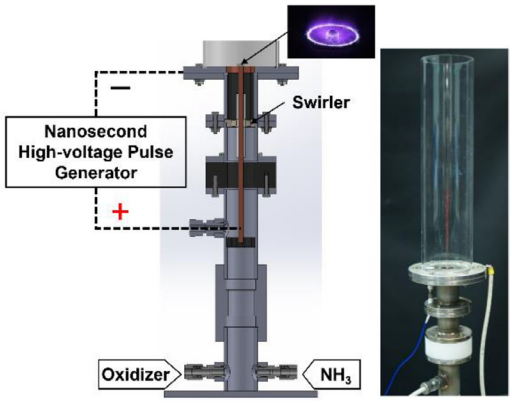

Fig. 1. Section view and photograph of the swirl stabilized dump combustor.

The ammonia/air mixture passes through an annular axial swirler. The swirler has 12 vanes with a trailing edge angle of 35°, and the hub and outer swirler diameters are 11 mm and 19 mm, respectively. The swirl number is 0.57 which is calculated from the following equation [10]:

$$S_N = \frac{2}{3} \times \frac{1-(D_{hub}/D_{sw})^3}{1-(D_{hub}/D_{sw})^2} \tan\theta$$

where D_{hub} is the hub diameter, D_{sw} is the outer swirler diameter and θ is the vane angle. Turbulent premixed flames are confined in a quartz tube with an inner diameter of 70 mm and a length of 305 mm.

A high-voltage pulse generator (FID Technologies FPG 50–50MC2) producing nano-second high voltage pulse is connected between the central electrode inside the injection tube and the outer ring at the injector exit as shown in Fig. 1. The anode is the central copper electrode with a diameter of 5 mm, and the rim of the injection tube with an inner diameter of 19 mm is the cathode. The voltage and current waveforms are measured by a high-voltage probe (Lecroy PPE 20 kV) and a Pearson coil (model 6585), respectively. The pulse repetition frequency (f) and peak voltage amplitude (V) can be independently adjusted. The full width at half maximum (FWHM) of the voltage waveform is 22 ns which is independent of the pulse repetition frequency and peak voltage. The power of plasma (P) can be determined by integrating the voltage and the conduction current over time. The details of the experimental setup and characteristics of nano-second pulsed plasma used in this study can be found in our previous work [10].

NH_2 is a key species in ammonia oxidation [4] and NO_x reduction [19]. Even though the relationship between NH_2 and NH_2^* is not clear, NH_2^* chemiluminescence may be used as an indicator of NH_2 production [20]. Thus, NH_2^* chemiluminescence near 630 nm (α-band) [9,21,22] is measured with a bandpass filter centered at 632 nm with ±5 nm FWHM using a digital DSLR camera (Sony A55) or a CMOS camera (NAC GX-3) equipped with an intensifier (Ultracam3).

It is well known that OH radicals accelerate ammonia decomposition to NH_2 [16]. Therefore, OH PLIF measurements are also performed. An Edge-wave (IS300–2-L) Nd:YAG laser (532 nm and 12 mJ/pulse) operating at 2.5 kHz is used to pump a Sirah Creedo dye laser (CREEDO-DYE-N) which passes the 532 nm beam through Rhodamine-6 G dye to convert the wavelength to 565.8 nm. The converted beam then passes through a frequency doubling crystal to change the wavelength to 282.9 nm. The dye laser (0.6 mJ/pulse) is tuned to the $Q_1(6)$ line of the $A^2\Sigma+ \rightarrow X^2\Pi$ (1, 0) band of OH at approximately 282.9 nm and the output of pulse energy is monitored using a photodiode. The laser beam is expanded into a sheet of 76 mm in height from the dump plane and approximately 0.5 mm thick using a two-lens telescope. Fluorescence from the OH(A–X) (1, 0) and (0, 0) bands [14] is captured with a bandpass filter centered at 320 nm with ±20 nm FWHM and image onto a CMOS camera (NAC GX-3) equipped with an intensifier (Ultracam3). The intensifier and the laser are synchronized at 2.5 kHz. In all NH_2^* chemiluminescence and OH PLIF measurements, the oxidizer flow rate is fixed at 608 cm^3/s. The emission from the discharge is blacked out by a knife edge to improve signal-noise ratio.

3. Results and discussion

3.1. Broadband chemiluminescence with and without plasma

In this study, flame morphology and location of premixed ammonia/air flames are investigated by observing broadband chemiluminescence from the flame. The location of flame is critical in the design of gas turbine combustors because lifted flames cause safety concerns.

Fig. 2 shows a flame stability map depending on air flow rate and equivalence ratio. A general observation from Fig. 2 is that plasma can extend the lean limits at which flame attaches to the burner exit to improve the flame stability. The operating conditions for representative cases of the flame stability map are shown in Table 1. The thermal loading is calculated using the lower heating value of ammonia (18.6 MJ/kg) [4] based on the fuel flow rate. The Reynolds number is calculated as: $Re \equiv UD/\nu$ where U is an averaged jet exit velocity, D is the hydraulic diameter of the burner exit and ν is the kinematic viscosity of the mixture.

Figs. 3 and 4 show the broadband chemiluminescence of ammonia flames with and without plasma at different conditions. Specifically, Fig. 3 presents the effects of plasma discharges on

Please cite this article as: J. Choe and W. Sun, Experimental investigation of non-equilibrium plasma-assisted ammonia flames using NH2* chemiluminescence and OH planar laser-induced fluorescence, Proceedings of the Combustion Institute, https://doi.org/10.1016/j.proci.2022.07.001

Table 1
Operating conditions for cases (a)–(d).

Condition	(a)	(b)	(c)	(d)
Jet exit velocity [m/s]	2.91	2.82	2.76	2.73
Reynolds number	2742	2647	2592	2557
Air flow rate [cm^3/s]	608	608	608	608
NH_3 flow rate [cm^3/s]	160	136	121	112
Equivalence ratio (ϕ)	0.94	0.80	0.71	0.66
Thermal loading of flame [kW]	2.08	1.76	1.57	1.45
Swirl number	0.57	0.57	0.57	0.57

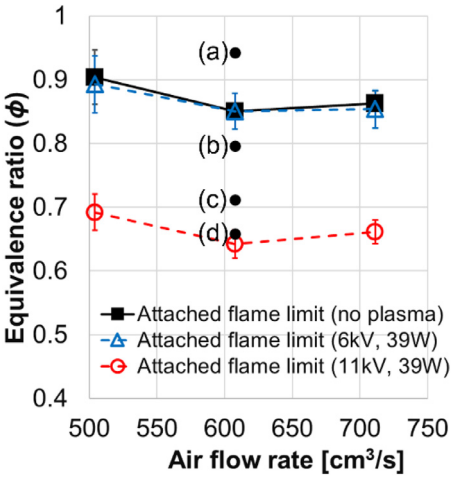

Fig. 2. Attached flame limits with and without plasma.

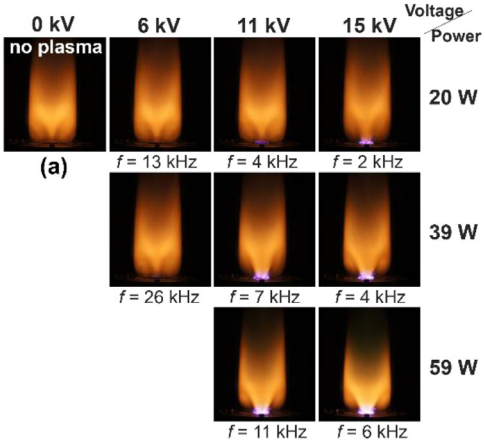

Fig. 3. Broadband chemiluminescence (ISO100, F/10, 2 s) without and with plasma in case (a) of Table 1.

the morphology of broadband chemiluminescence at $\phi = 0.94$. Without plasma activation, stable orange colored flames are observed at both the inner shear layer (ISL, "V" shape of flame) and the outer shear layer (OSL, outside of "V" shape) at the equivalence ratio of 0.94, as shown in Fig. 3(a) (corresponding to the condition marked (a) in Fig. 2). When the equivalence ratio is decreased below 0.85, flames are lifted from the dump plane (Fig. 4(b) and (c)). With the further decrease in equivalence ratio below the lean blowoff limit, blowoff occurs, and the flame extinguishes.

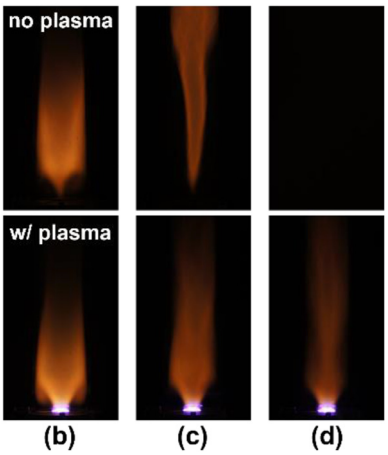

Fig. 4. Broadband chemiluminescence (ISO100, F/10, 2 s) without and with plasma ($V = 11$ kV, $f = 7$ kHz, $P = 39$ W) in cases (b)-(d) of Table 1.

As the discharge voltage and power increase, flames become vigorous at ISL. When plasma discharges with a peak voltage of 11 kV and repetition frequency of 7 kHz are generated in the lifted flame regime, lifted flames attach to the burner exit as shown in Fig. 4. At this plasma condition, discharge power is 39 W which is corresponding to only 1.9% of thermal load in case (a) of Table 1. With this plasma condition ($V = 11$ kV, $P = 39$ W), the attached flame regime significantly extends to the red dashed line from the black solid line as shown in Fig. 2. However, when the peak voltage is decreased to 6 kV ($f = 26$ kHz) keeping the plasma power of 39 W constant, the effect of plasma on the extension of the attached flame region is negligible. It was reported that extensions of lean blowoff limits were most sensitive to discharge voltage and 39 W thermal power only increased the average reactant temperature by 6 K in the previous work

Please cite this article as: J. Choe and W. Sun, Experimental investigation of non-equilibrium plasma-assisted ammonia flames using NH2* chemiluminescence and OH planar laser-induced fluorescence, Proceedings of the Combustion Institute, https://doi.org/10.1016/j.proci.2022.07.001

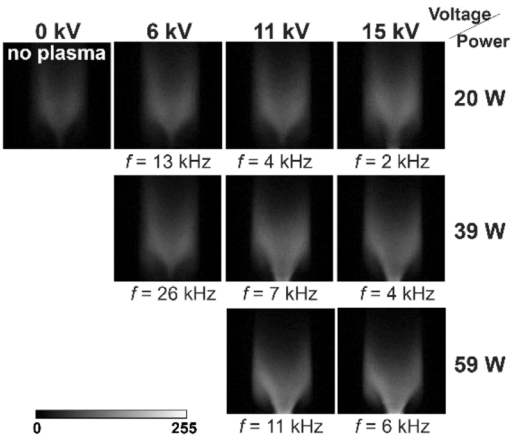

Fig. 5. Effects of discharge voltage and power on averaged NH_2^* chemiluminescence (2 s).

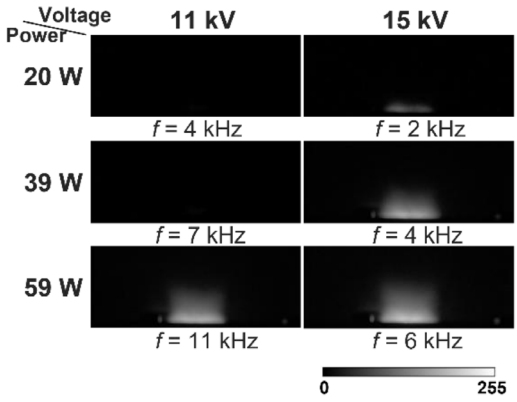

Fig. 6. Effects of plasma properties on averaged NH_2^* chemiluminescence (2 s) at $\phi = 0.48$.

[18]. It was concluded that the effects of plasma on lean blowoff limits were kinetic mainly. Thus, the mechanism of flame attachment may also be a kinetic effect.

3.2. NH_2^* chemiluminescence with and without plasma

Fig. 5 presents the averaged images (2 s) of NH_2^* chemiluminescence at condition (a) in Table 1. Compared to broadband chemiluminescence (Fig. 3), the signal of NH_2^* chemiluminescence in OSL is relatively weak. As the peak voltage and the plasma power are increased, the signal becomes more intense at ISL, especially near the plasma discharge regime. This indicates more production of NH_2^* by plasma. It is observed that the effect of voltage is more significant than that of the discharge power. At 6 kV, although the discharge power increases from 20 W to 39 W, the change of morphology and the intensity of NH_2^* chemiluminescence are very limited. However, when the discharge voltage is increased from 6 kV to 15 kV but keeping the discharge power constant at 39 W, NH_2^* chemiluminescence near the discharge region is significantly stronger and shows a clear "V" shape (ISL flame). The effects of discharge voltage on NH_2^* chemiluminescence at constant discharge power may be explained by the change of the reduced electric field, E/N, where E is the electric field and N is the particle number density. Higher E/N value modifies the pathways of energy deposition and more energy can be used for the generation of radicals [10]. However, the reaction pathways of plasma/NH_3 interaction are largely unknown. Future detailed investigation on the fundamentals is warranted.

The power of plasma also affects the intensity of NH_2^* chemiluminescence. For example, at 15 kV, the signals near the discharge region become brighter as the plasma power increases (Fig. 5). The increase of plasma power with the same voltage is accomplished by the increase of pulse repetition frequency. Thus, higher frequency means the increase of total energy deposition into the gas mixture which could generate more radicals.

To further verify NH_2^* production from the plasma, experiments are conducted in a very lean condition ($\phi = 0.48$, no visible flame existed) with different plasma properties as shown in Fig. 6. It is clearly seen that plasma itself can generate NH_2^* chemiluminescence without the help of visible flame. The effects of voltage and the power of plasma are similar to the condition with flame presented in Fig. 5. Higher voltage results in stronger NH_2^* chemiluminescence and it becomes more intense with the increase of plasma power at constant discharge voltage of 15 kV. The tendency that NH_2^* chemiluminescence increases with plasma power and voltage is the same as that of NO_x reduction with plasma in the previous work [18]. Pugh et al. [8] also observed NO_x reduction with increase in NH_2^* chemiluminescence when they increased the equivalence ratio. It is possible that NO is consumed through reactions with NH_2: $NO+NH_2 \rightarrow NNH+OH$ and $NH_2+NO \rightarrow N_2+H_2O$ in the thermal De-NO_x process [18,19]. Therefore, NO_x reduction in the presence of plasma might be related to additional NH_2 production from the plasma.

Fig. 7 shows the effects of ammonia concentration on NH_2^* chemiluminescence and morphology of plasma discharge. As the equivalence ratio is increased from 0 to 0.48, NH_2^* chemiluminescence intensity increases with the increase of ammonia concentration. At the same time, qualitative change on discharge morphology was observed through time integrated photographs as shown in Fig. 7. Without ammonia, discharge only exists near the center of the electrodes. With the addition of ammonia, discharge becomes significantly

Please cite this article as: J. Choe and W. Sun, Experimental investigation of non-equilibrium plasma-assisted ammonia flames using NH2* chemiluminescence and OH planar laser-induced fluorescence, Proceedings of the Combustion Institute, https://doi.org/10.1016/j.proci.2022.07.001

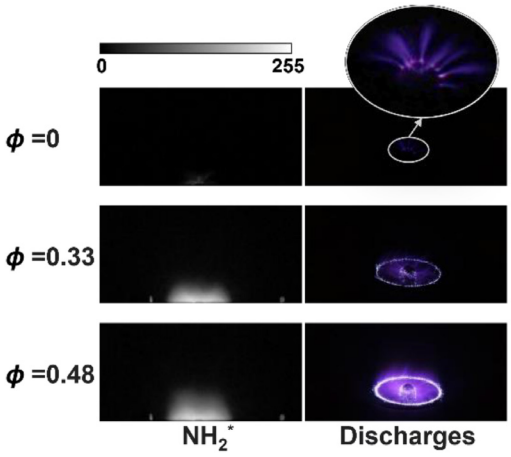

Fig. 7. Effects of equivalence ratio on averaged NH_2^* chemiluminescence (2 s) with plasma ($V = 15$ kV, $P = 39$ W) and corresponding direct photographs of plasma discharges.

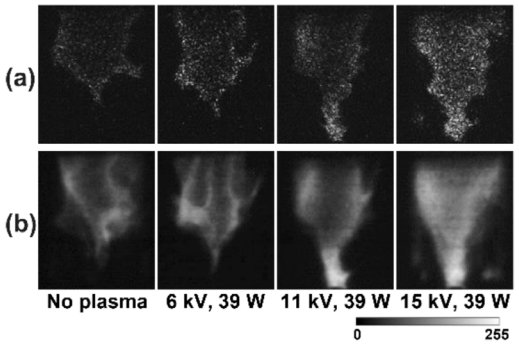

Fig. 8. (a) Instantaneous and (b) averaged OH PLIF images without and with plasma at condition (a) in Table 1.

brighter filling between the electrodes. This might be related to the change of flow temperature and composition owing to the oxidation of NH_3. Further studies are required in the future to reveal the change of discharge properties.

3.3. OH PLIF with and without plasma

To further understand flame stabilization mechanism, OH PLIF measurement is conducted. Fig. 8 presents the instantaneous and averaged OH PLIF images at condition (a) in Table 1. Averaged images are integrated over 400 measurements. Without plasma, OH PLIF signal only exists in the flame (away from the nozzle) and inner recirculation region. When the plasma is activated at $V = 6$ kV and $P = 39$ W, there is no significant change between cases without and with plasma. If the voltage is increased to 11 kV while keeping the plasma power constant at 39 W, intense OH PLIF signals

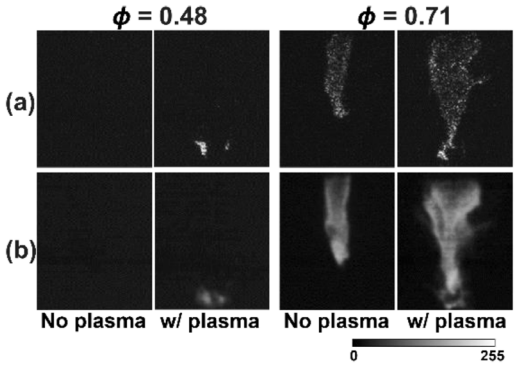

Fig. 9. (a) Instantaneous and (b) averaged OH PLIF images without and with plasma ($V = 15$ kV, $P = 39$ W) at $\phi = 0.48$ (left) and $\phi = 0.71$ (right).

appear near the discharge region (exit of the injection tube). With the voltage of 15 kV, not only near the discharge region but also the entire flame shows intense OH PLIF signals. The OH PLIF signal morphology with and without plasma activation is very similar to that of NH_2^* chemiluminescence shown in Fig. 5.

With equivalence ratio of 0.71, ammonia flame without plasma is lifted from the injection tube as shown in Fig. 9. With plasma application, the flame attached to burner exit and intense OH PLIF signals are observed near the exit of injection tube. When the equivalence ratio is decreased to 0.48 with plasma activation, the intense flame no longer exists but OH PLIF signals still appear near the discharge region as shown in Fig. 9. Clearly, plasma discharges generate OH radicals which help to stabilize the flame.

3.4. The relation between OH and NH_2^* in ammonia oxidation with plasma

To understand the relationship between OH and NH_2^* in the presence of plasma discharge, time-averaged OH PLIF and Abel-inverted distribution of NH_2^* chemiluminescence images are overlapped. It is noted that the NH_2^* chemiluminescence is axisymmetric only in time averaged results but asymmetric in instantaneous images. Therefore, the Abel-inverted distribution of NH_2^* chemiluminescence is only used for qualitative explanation. The corresponding images are presented in Fig. 10. To improve the signal-to-noise ratio near the discharge area, the gain of the intensifier is increased by 50% compared to previous measurements. At equivalence ratio 0.57, both OH PLIF and NH_2^* chemiluminescence signals are presented near the discharge region and NH_2^* chemiluminescence distributed in the outer edge of the OH PLIF regime. When the equivalence ratio increases to 0.64 (lifted flame), OH PLIF and NH_2^* chemiluminescence

Please cite this article as: J. Choe and W. Sun, Experimental investigation of non-equilibrium plasma-assisted ammonia flames using NH2* chemiluminescence and OH planar laser-induced fluorescence, Proceedings of the Combustion Institute, https://doi.org/10.1016/j.proci.2022.07.001

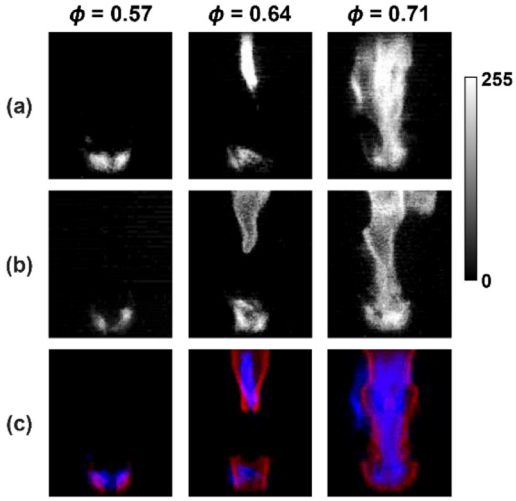

Fig. 10. Averaged (100 ms) (a) OH PLIF, (b) raw NH_2^* chemiluminescence and (c) overlapped images (blue: OH PLIF, red: Abel-inverted distribution of NH_2^* chemiluminescence) with plasma ($V = 11$ kV, $P = 39$ W).

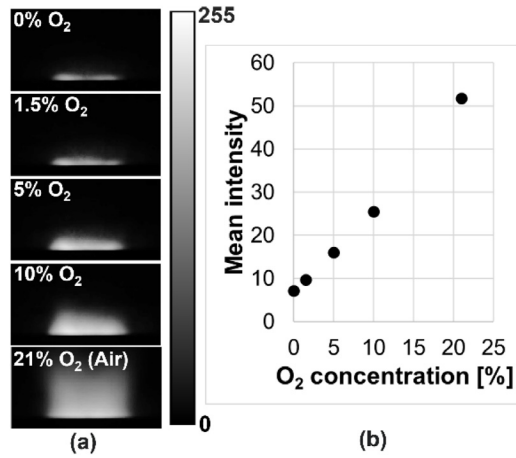

Fig. 11. (a) Averaged NH_2^* chemiluminescence (2 s) and (b) mean intensity of each image depending on O_2 concentration with plasma ($V = 11$ kV, $P = 59$ W).

signals exist near the discharge region as well as lifted flames even though these two regimes are disconnected. As the equivalence ratio further increases to 0.71, lifted flams are attached to the injection tube and OH PLIF and NH_2^* chemiluminescence signals are observed in both the discharge region and flames which are connected. Still, NH_2^* chemiluminescence distributes in the outer edge of OH PLIF regime near flame front. As shown in Fig. 10, there are discrepancies between the features of NH_2^* chemiluminescence and OH PLIF. This is because one is line-of-sight and one is planar, and they are not captured simultaneously neither. Moreover, discharges occurred randomly between two electrodes and the location of OH signal near discharge region could be random.

To further understand the relationship between OH and NH_2^*, oxygen (O_2) in air is replaced by nitrogen (N_2) with the total flow rate (608 cm^3/s) unchanged when equivalence ratio is at $\phi = 0.57$. With discharge voltage at 11 kV and discharge power at 39 W, no measurable NH_2^* chemiluminescence signal is detected. The plasma power is then increased to 59 W and weak NH_2^* chemiluminescence can be observed as shown in Fig. 11(a). If oxygen is added into the flow (with different mole fractions), NH_2^* chemiluminescence increases almost linearly with the mole fraction of O_2 in the flow as presented in Fig. 11(a) and (b). In Fig. 11(b), the mean intensity value is obtained by integrating the histogram of each image and dividing it by the number of pixels. This implies that plasma itself can generate NH_2^* through electron impact reactions, but such production is very limited. Addition of O_2 greatly enhances the production of NH_2^* very possibly owing to the production of OH and O which could subsequently react with NH_3 to produce NH_2^*.

4. Conclusion

In this work, the effect of nano-second pulsed plasma on premixed ammonia/air flames is investigated using a model gas turbine combustor. Broadband chemiluminescence, NH_2^* chemiluminescence, and OH PLIF measurements are conducted to understand the effect of plasma on flame stabilization. It is found that plasma can extend the attached flame regime to a much lower equivalence ratio. At equivalence ratio of 0.94, both NH_2^* chemiluminescence and OH PLIF signals near the discharge region become significantly more intense with the activation of plasma. Both NH_2^* chemiluminescence signal and OH PLIF signal increase with the increase of discharge voltage and power. At very lean conditions ($\phi = 0.48$–0.57, no existing visible flame), NH_2^* chemiluminescence and OH PLIF signals near the injection tube can be observed which implies that plasma produces NH_2^* and OH radicals.

Based on the observation that (1) NH_2^* chemiluminescence distributes in the outer edge of OH PLIF regime and (2) When air is replaced by nitrogen in the experiments, NH_2^* chemiluminescence is very weak but measurable at a higher discharge power ($P = 59$ W). If O_2 is gradually added into the mixture, NH_2^* chemiluminescence signal increases with the increase of O_2 concentration in the mixture. Thus, OH or oxygen-related species, such as atomic O, may play an important role in the generation of NH_2^* in the presence of plasma discharges. Better understanding of the relationship between

Please cite this article as: J. Choe and W. Sun, Experimental investigation of non-equilibrium plasma-assisted ammonia flames using NH2* chemiluminescence and OH planar laser-induced fluorescence, Proceedings of the Combustion Institute, https://doi.org/10.1016/j.proci.2022.07.001

OH and NH_2 requires simultaneous OH and NH_2 PLIF measurements in the future.

Further fundamental studies, such as quantitative measurements in a flow reactor, are also needed to understand the mechanism of NH_2 production with plasma activation in ammonia containing mixtures.

Declaration of Competing Interest

None

Acknowledgments

This work is supported by the National Science Foundation under Grant No. 2002836.

References

[1] U.S. Army Engineer Research and Development Laboratories, *Development of an Ammonia Burning Gas Turbine Engine*, Fort Belvoir, Solar, 1968 DA-44-009 AMC-824(T).
[2] O. Kurata, N. Iki, T. Inoue, T. Matsunuma, T. Tsujimura, H. Furutani, M. Kawano, K. Arai, E. Okafor, A. Hayakawa, H. Kobayashi, *Proc. Combust. Inst.* 37 (2019) 4587–4595.
[3] F. Verkamp, M. Hardin, J. Williams, *Symp. Int. Combust.* 11 (1967) 985–992.
[4] H. Kobayashi, A. Hayakawa, K. Somarathne, E. Okafor, *Proc. Combust. Inst.* 37 (2019) 109–133.
[5] O. Kurata, N. Iki, T. Matsunuma, T. Inoue, T. Tsujimura, H. Furutani, H. Kobayashi, A. Hayakawa, *Proc. Combust. Inst.* 36 (2017) 3351–3359.
[6] A. Valera-Medina, R. Marsh, J. Runyon, D. Pugh, P. Beasley, T. Hughes, P. Bowen, *Appl. Energy* 185 (2017) 1362–1371.
[7] D. Pugh, P. Bowen, A. Valera-Medina, A. Giles, J. Runyon, R. Marsh, *Proc. Combust. Inst.* 37 (2019) 5401–5409.
[8] D. Pugh, A. Valera-Medina, P. Bowen, A. Giles, B. Goktepe, J. Runyon, S. Morris, S. Hewlett, R. Marsh, *ASME Turbo Expo* (2020) GT2020–G14953 2020.
[9] D. Pugh, J. Runyon, P. Bowen, A. Giles, A. Valera-Medina, R. Marsh, B. Goktepe, S. Hewlett, *Proc. Combust. Inst.* 38 (2021) 6451–6459.
[10] J. Choe, W. Sun, *J. Phys. D Appl. Phys.* 51 (2018) 365201.
[11] D. Lacoste, J. Moeck, D. Durox, C. Laux, T. Schuller, *J. Eng. Gas Turb. Power* 135 (2013) 101501.
[12] W. Kim, J. Snyder, J. Cohen, *Proc. Combust. Inst.* 35 (2015) 3479–3486.
[13] W. Kim, J. Cohen, *Combust. Sci. Technol.* 193 (2019) 869–888.
[14] D. Lacoste, D. Xu, J. Moeck, C. Laux, *Proc. Combust. Inst.* 34 (2013) 3259–3266.
[15] R. Rajasegar, C. Mitsingas, E. Mayhew, S. Hammack, H. Do, T. Lee, *IEEE Trans. Plasma Sci.* 44 (2016) 39–48.
[16] A. Shioyoke, J. Hayashi, R. Murai, N. Nakatsuka, F. Akamatsu, *Energy Fuels* 32 (2018) 3824–3832.
[17] G. Faingold, J. Lefkowitz, *Proc. Combust. Inst.* 38 (2021) 6661–6669.
[18] J. Choe, W. Sun, T. Ombrello, C. Carter, *Combust. Flame* 228 (2021) 430–432.
[19] J. Miller, M. Pilling, J. Troe, *Proc. Combust. Inst.* 30 (2005) 43–88.
[20] R. d'Agostino, F. Cramarossa, S. De Benedictis, G. Ferraro, *Plasma Chem. Plasma Process.* 1 (1981) 19–35.
[21] V. Donnelly, A. Baronavski, J. McDonald, *Chem. Phys.* 43 (1979) 271–281.
[22] Y. Yi, X. Wang, A. Jafarzadeh, L. Wang, P. Liu, B. He, J. Yan, R. Zhang, H. Zhang, X. Liu, H. Guo, E. Neyts, A. Bogaerts, *ACS Catal.* 11 (2021) 1765–1773.

Please cite this article as: J. Choe and W. Sun, Experimental investigation of non-equilibrium plasma-assisted ammonia flames using NH2* chemiluminescence and OH planar laser-induced fluorescence, Proceedings of the Combustion Institute, https://doi.org/10.1016/j.proci.2022.07.001